Learning from the path not taken: Sensory prediction error computation and implicit motor adaptation proceed without movement

Olivia A. Kim[1], Alexander D. Forrence[2], and Samuel D. McDougle[2]

1. Department of Psychology, Princeton University, Princeton, NJ 08544
2. Department of Psychology, Yale University, New Haven, CT 06511

Correspondence to:
Olivia Kim
oakim@princeton.edu
kim.olivia.a@gmail.com

Number of Pages: 29
Number of Figures in Main Text: 3
Number of Supplemental Figures: 4
Number of Supplemental Tables: 3
References: 60 (45 main text, 15 methods-only)
Number of Characters (including spaces):
Abstract (1,293)
Highlights (306)
Main text, including main figure legends (27,858)
Methods (15,013)

AUTHOR CONTRIBUTIONS
Conceptualization, OK, AF, & SM; Methodology, OK, AF, & SM; Software, OK & AF; Validation, OK & AF; Formal Analysis, OK & AF; Investigation, OK & AF; Resources, OK & SM; Data Curation, OK & AF; Supervision, SM; Project Administration, SM; Funding Acquisition, OK & SM; Writing – original draft, OK; Writing – review & editing, OK, AF, & SM

CONFLICT OF INTEREST
The authors declare no competing financial interests.

ACKNOWLEDGEMENTS
This work was supported by a grant from the National Institutes of Health to OK (F32-NS122921).

ABSTRACT

Prediction errors guide many forms of learning, providing teaching signals that help us improve our performance. Implicit motor adaptation, for instance, is driven by sensory prediction errors (SPEs), which occur when the expected and observed consequences of a movement differ. Traditionally, SPE computation is thought to require movement execution. However, recent work suggesting that the brain generates and accounts for sensory predictions based on motor imagery or planning alone calls this assumption into question. Here, by measuring implicit adaptation during a visuomotor task, we tested whether motor planning and well-timed sensory feedback are sufficient for SPE computation. Human participants were cued to reach to a target and were, on a subset of trials, rapidly cued to withhold these movements. Errors displayed both on trials with and without movements induced single-trial implicit learning. Learning following trials without movements persisted even when movement trials had never been paired with errors, and when the direction of movement and sensory feedback trajectories were decoupled. These observations demonstrate that the brain can compute SPEs without generating overt movements, leading to the adaptation of planned movements even when they are not performed.

HIGHLIGHTS

- The brain can learn to update movements that are not performed, representing a mechanism for learning based only on movement planning and sensory expectation.
- Supports a fundamental role for prediction in adaptation.
- Provides further support for the role of forward models in predictive motor control.

KEYWORDS

predictive coding, forward model, mental imagery, supervised learning

INTRODUCTION

Prediction errors help to optimize behavior by driving learning processes that correct for our mistakes. Accordingly, they are thought to be a fundamental computation of the nervous system.[1] Specific types of prediction errors are associated with specific learning processes, and sensory prediction errors (SPEs) are the teachers of the implicit motor system, triggering adaptation and refinement of movements.[2–6] Traditionally, SPEs are thought to be computed by comparing the expected and observed consequences of a movement, with movement execution being a critical element in this process.[4,7] However, the predictions factoring into SPE computation are thought to be generated by an internal forward model, which estimates the consequences of movements before relevant sensory feedback can reach the brain.[7] This predictive capacity suggests that the forward model predicts the sensory consequences of an intended movement regardless of whether that movement occurs. That is, because movements are synchronous with the sensory outcomes that they produce, motor execution cannot itself be necessary for the generation of predictions by the forward model.

Recent work supports the claim that the brain generates predictions related to the sensory consequences of movements before they can be performed, and even when there is never any intention to move.[9–12] Considering that these studies imply that movements are not needed for the generation of sensorimotor predictions, it may be that these predictions can be combined with sensory observations to support SPE computation without actual motor execution. In other words, SPEs should be effectively computed based upon only two events – generation of a sensory prediction and observation of sensory feedback (**Fig. 1a**). Here, we used implicit motor adaptation as a readout for SPE occurrence, as SPEs are both necessary and sufficient for this form of learning, and asked if motor planning and subsequent sensory events are sufficient to drive SPE computation without movement.[5,13–18] While prior work has illustrated that cognitive processes support visuomotor learning without movement by observers who witnesses others' motor errors, these processes may be recruited by performance errors beyond SPE, or by a combination of multiple sources of error and multiple learning processes.[19–21] Here, we isolate implicit motor learning to specifically test whether SPE computation requires movement execution.

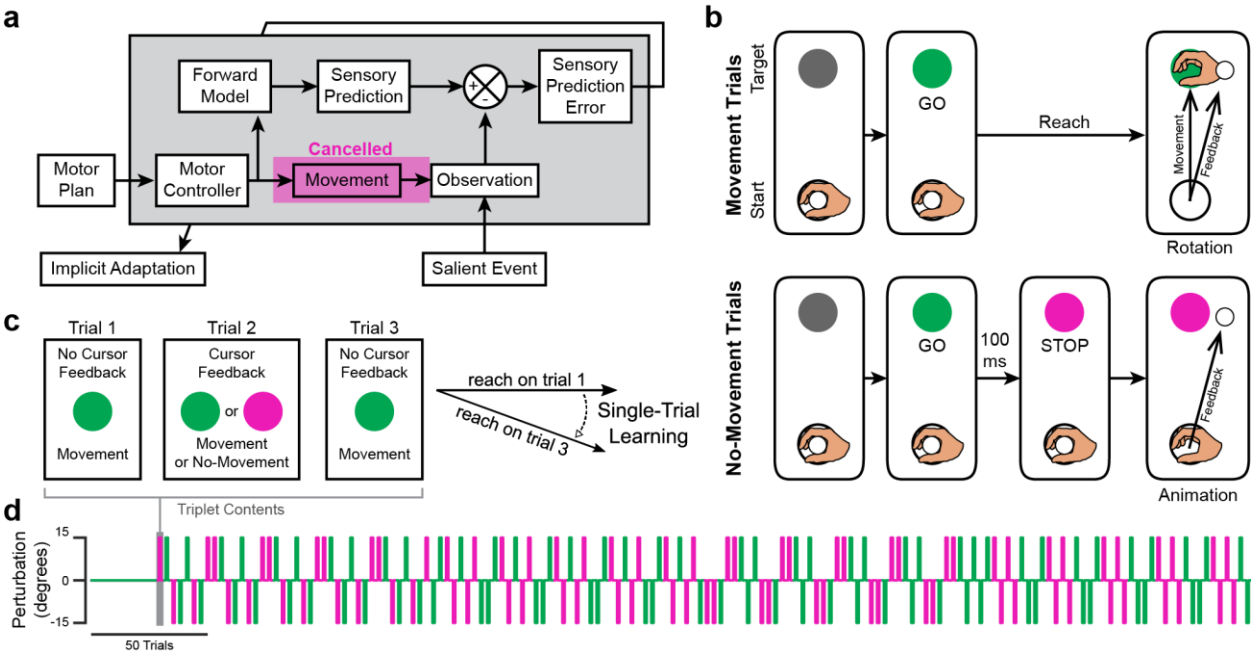

Figure 1. Schematics showing the proposed learning framework and task design. (**a**) Schematic showing how the forward model may support implicit motor adaptation in the presence of sensory feedback not causally related to self-generated movement. (**b**) Schematic of events on trials with visual feedback. The robotic apparatus brought the participant's hand to the starting location to initiate a trial. On Movement trials (top), the target turned green ('GO'), cueing participants to reach through the target. On trials with visual feedback, participants observed a white feedback cursor move along a rotated trajectory ('Rotation'). On No-Movement trials (bottom), the target turned magenta 100 ms after turning green, cueing participants to withhold movement ('STOP'). After a delay, an animation showing the feedback cursor moving 15° off-target played ('Animation'). The hand is shown in the figure for illustrative purposes but was not visible during the experiment. (**c**) Schematic showing the trials that constituted a triplet and how single-trial learning (STL) was computed. Triplets were composed of 2 Movement trials without visual feedback flanking either a Movement or a No-Movement trial with visual feedback. STL was measured as the difference between reach angles on the flanking trials. (**d**) Schematic showing the pseudorandomized order in which trials were presented for an example participant, with color reflecting the movement condition (Movement: green, No-Movement: magenta).

We measured trial-by-trial implicit adaptation during a visuomotor task in which human participants saw visual feedback while performing – or withholding – hand and arm movements, using a modified stop-signal paradigm. At the onset of each trial, a "Go" cue was presented, instructing participants to make a movement through a visual target. On some trials, a "Stop" cue was presented shortly after presenting the "Go" cue, instructing participants to withhold the movement ("No-Movement" trials, **Fig. 1b**). We reasoned that presenting the "Go" cue on "Stop" trials would be a sufficient stimulus to induce prediction generation and support sensory prediction error computation, given that prior work has shown that cued – but ultimately withheld – movements can still serve as an input to a forward model and support the generation of

differential sensory predictions.[12] To isolate implicit adaptation, we employed a recently-developed approach that requires participants to aim their movements directly for presented targets and disregard visual feedback.[17,22–26] We predicted that single-trial motor adaptation would occur following both typical movement (Go) trials that generated sensory error, as well as trials where movements were withheld (Stop) but "simulated" sensory errors were observed. If confirmed, this result would demonstrate that SPEs can be computed in the absence of movement and can cause adaptation of planned but not performed movements. Furthermore, such a result would provide strong support for predictive models of motor adaptation.

RESULTS

Simulated and typical visuomotor rotations cause motor adaptation

In our first study, we measured implicit motor adaptation in humans (n = 20) performing straight reaches during a visuomotor adaptation task (**Fig. 1b**). Vision of the hand and arm was occluded by a mirror that reflected visual feedback from a horizontally mounted monitor. A white cursor provided feedback about participants' hand positions as they reached from a starting location to a displayed target. After a brief acclimation period, trials were organized into triplets, such that each trial with cursor feedback was flanked by trials without cursor feedback. This allowed for a reliable measurement of single-trial learning (STL) in response to feedback, quantified as the difference between hand angles on the first and third trials of each triplet (**Fig. 1c**). Trials with cursor feedback were either "Movement" trials on which a "Go" signal prompted movement or No-Movement trials on which a "Stop" signal indicated that movements should be withheld. On Movement trials, feedback involved a visuomotor error (±15° rotation added to the visual cursor path; + = clockwise; **Fig. 1b right**). On No-Movement trials, sensory feedback involved a simulation of the cursor's path, using timing variables based on ongoing measurements of participant behavior (see *Methods*). All flanking trials of each triplet were "Go" trials and thus required movements. The direction of the error (clockwise [CW] or counterclockwise [CCW]) was pseudorandomly varied across triplets to maintain overall adaptation near 0 throughout the session (**Fig. 1d**). This straightforward design allowed us to test the hypothesis that SPE computation and motor adaptation do not require movement and sensory feedback to be causally linked (**Fig. 1a**).

Consistent with our predictions, rotated cursor paths on Movement and No-Movement trials both caused subsequent hand trajectories to shift opposite the direction of the rotation (**Fig. 2b**-**c**), with a two-way repeated measures ANOVA revealing statistically significant main effects of the direction (CW vs CCW) of the perturbation applied ($F(1, 19) = 98.62$, $p = 5.89 \times 10^{-9}$, $\eta_G^2 = 0.76$). While there was no significant main effect of withholding movement ($F(1, 19) = 1.79$, $p = 0.20$), we observed a significant interaction between the perturbation applied and withholding movement ($F(1, 19) = 137.32$, $p = 3.87 \times 10^{-10}$, $\eta_G^2 = 0.49$). Post-hoc pairwise comparisons confirmed that STL was sensitive to perturbation direction during both Movement (paired t-test: $t(19) = 12.92$, $p_{adj} = 2.96 \times 10^{-10}$, *Cohen's d* = 5.12) and No-Movement triplets ($t(19) = 4.39$, $p_{adj} = 3.13 \times 10^{-4}$, *Cohen's d* = 1.63), and indicated that STL magnitude was greater across Movement than No-Movement triplets (paired-samples signed-rank test, CW rotations: $V = 210$, $p_{adj} = 2.55 \times 10^{-6}$, $r = 0.88$; CCW rotations: $t(19) = 9.43$, $p_{adj} = 2.70 \times 10^{-8}$, *Cohen's d* = 2.02) rotations. However, we note that the amplitude of adaptation observed both with and without movement was within the range of implicit learning rates measured in previous visuomotor rotation studies (**Supplemental Fig. 1**).

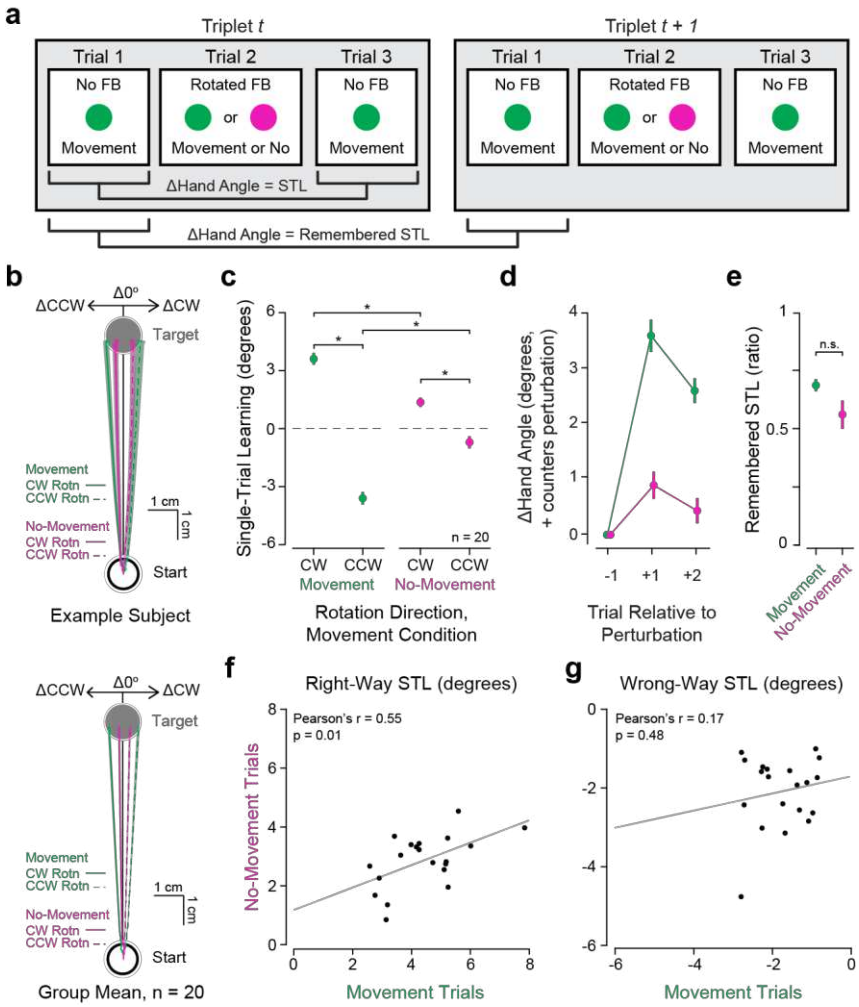

Figure 2. Effects of typical and simulated errors during a visuomotor reach adaptation task. (**a**) Schematic illustrating how STL and remembered STL measurements were computed. (**b**) An example subject's (top) and the group's (bottom) mean ± SEM changes in reach paths across triplets with a rotation applied (green: triplets with perturbations on Movement trials, magenta: triplets with perturbations on No-Movement trials, solid lines: perturbation was a CW rotation, dashed lines: perturbation was a CCW rotation). (**c**) STL across Movement (green) and No-Movement (magenta) triplets for all participants (n = 20). In the reference frame used here, positive changes in hand angle are CCW. Please refer to Supplemental Table 1 for details on all statistical tests. (**d**) Group mean ± SEM Δhand angle values after exposure to Movement (green) and No-Movement (magenta) trial perturbations. Positive Δ values indicate that the change in hand angle proceeded opposite the direction of the perturbation (*i.e.,* the direction that would counter the error, "Right-Way"). (**e**) Group mean of participants' ratios of remembered STL to initial STL during Movement and No-Movement trials. (**f**) The relationship between Right-Way STL observed during Movement and No-Movement triplets. (**g**) As in (**f**), but for STL observed on trials where adaptation proceeded in the direction that would exacerbate the error (*i.e.*, the same direction as the perturbation applied, "Wrong Way"). Statistical significance (* = $p_{adj} < 0.05$; n.s. = $p_{adj} \geq 0.05$) is indicated. Abbreviations: STL – single-trial learning, CW – clockwise, CCW – counterclockwise, Δ – change in.

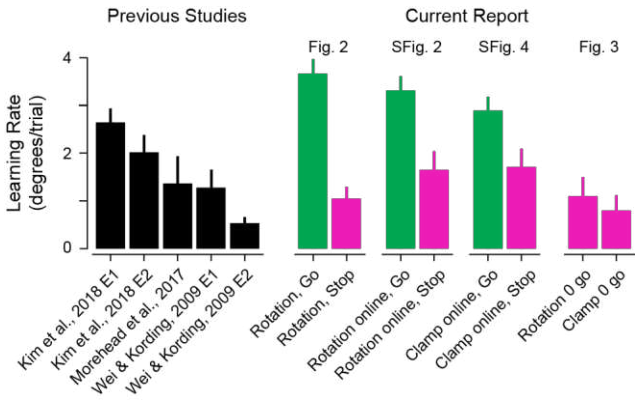

Supplemental Figure 1. Learning rates reported in the literature and observed in the current study. Learning rates for motor adaptation observed in previous studies are shown at left in black, and learning rates observed in each experiment in the current report are shown at the right, with data from Movement triplets shown in green and data from No-Movement triplets shown in magenta. Data are shown as mean ± SEM, and are shown for rotational/error clamp perturbations of 15°, with the exception of Wei & Kording, 2009 E2, where an 11° perturbation was applied. Papers referred to and their corresponding reference numbers: Kim et al., 2018[23]; Morehead et al., 2017[17]; Wei & Körding, 2009[27]. "Rotation, Go" and "Rotation, Stop" show data from the in-lab experiment where participants saw 15° rotated feedback on Movement trials (i.e., data from Fig. 2), "Rotation online, Go" and "Rotation online, Stop" show data from the online experiment where participants saw 0-15° rotated feedback on Movement trials (i.e., data from Supplemental Fig. 2). "Clamp online, Go" and "Clamp online, Stop" show data from the online experiment where participants saw 0-15° error-clamed feedback (i.e., data from Supplemental Fig., 4). "Rotation 0 go" and "Clamp 0 go" show data from the online experiments where participants saw 0° perturbed feedback on Movement trials. Abbreviations: E, experiment.

To address whether the STL measured represented genuine implicit learning, we checked whether adaptation persisted beyond the trial after an error was experienced. We examined participants' hand angles on the second trial after a perturbation relative to the pre-perturbation baseline trial (i.e., hand angle on trial 1 of triplet *t + 1* relative to hand angle on trial 1 of triplet *t,* subsequently referred to as remembered STL, **Fig. 2a**). Because visual feedback was withheld on both trial types, this approach provided a pure measure of persistent memory in the absence of error-driven changes in performance. Hand angle remained adapted in the direction opposite the rotation on trials with nonzero perturbations regardless of movement condition (**Fig. 2d**), suggesting that genuine implicit learning was observed in response to errors under both movement conditions. Closer examination of the relative ratio of remembered STL to initial STL revealed that retention of adaptation differed significantly from zero after both Movement ($t(19) = 26.20$, $p_{adj} = 6.71 \times 10^{-16}$, *Cohen's d* = 5.86) and No-Movement triplets ($t(19) = 9.20$, $p_{adj} = 2.98 \times 10^{-8}$, *Cohen's d* =

2.06). Moreover, the amount of retention observed was not statistically significantly different between the movement conditions ($t(19) = 2.07$, $p_{adj} = 0.053$, **Fig. 2e**).

To assess the potential similarity of mechanisms underlying adaptation after errors on Movement and No-Movement trials, we compared STL amplitude under each condition, reasoning that there should be a reliable relationship between the two measures if STL is supported by the same mechanism for both Movement and No-Movement trials. When we considered instances of STL in the direction that would compensate for the observed error (the direction opposite the rotation, i.e., the "Right-Way"), within-subject changes in hand angle were correlated between Movement and No-Movement trials (*Pearson's* $r = 0.55$, $p = 0.01$; **Fig. 2f**). Conversely, changes in hand angle in the direction that would exacerbate the observed error (the direction of the rotation, i.e., the "Wrong-Way") were uncorrelated between Movement and No-Movement trials (*Pearson's* $r = 0.17$, $p = 0.48$, **Fig. 2g**). Together, these observations suggest that the same learning process may underlie adaptive single-trial learning events in response to errors on both kinds of trials, while maladaptive changes in hand-angle may be attributable to noise.

Implicit motor adaptation proceeds after simulated errors in an online visuomotor task

Illustrating that the above observations are reproducible and generalize across experimental contexts, we again observed that simulated errors in No-Movement trials also induced motor adaptation in an online, crowd-sourced version of the task. Participants ($n = 40$) made hand movements using their computer mouse or trackpad to move a cursor towards a target. As in the experiment described above, trials were presented in triplets, allowing us to measure STL that occurred in response to cursor feedback presented during Movement and No-Movement trials at the center of each triplet (**Fig. 1b**-**d**). For this online study, triplets with 0° perturbations/simulated errors were also included to provide an estimate of baseline changes in hand angle, in the event that participants exhibited strong movement biases in the online platform.

Participants showed STL that was directionally appropriate for the perturbation applied during both Movement and No-Movement trials (**Supplemental Fig. 2a**-**c**, please refer to the supplemental material details of the statistical analysis). Further echoing the results of the in-person study, STL on both Movement and No-Movement trials was retained beyond the triplet in which the relevant error occurred (**Supplemental**

Fig. 2d-e), and the magnitude of STL in the direction that would counter the perturbation was again correlated across the two movement conditions (**Supplemental Fig. 2e**). These data provide further support for the claim that movements that are not performed can undergo implicit motor adaptation and extend our findings to a task with different movement demands.

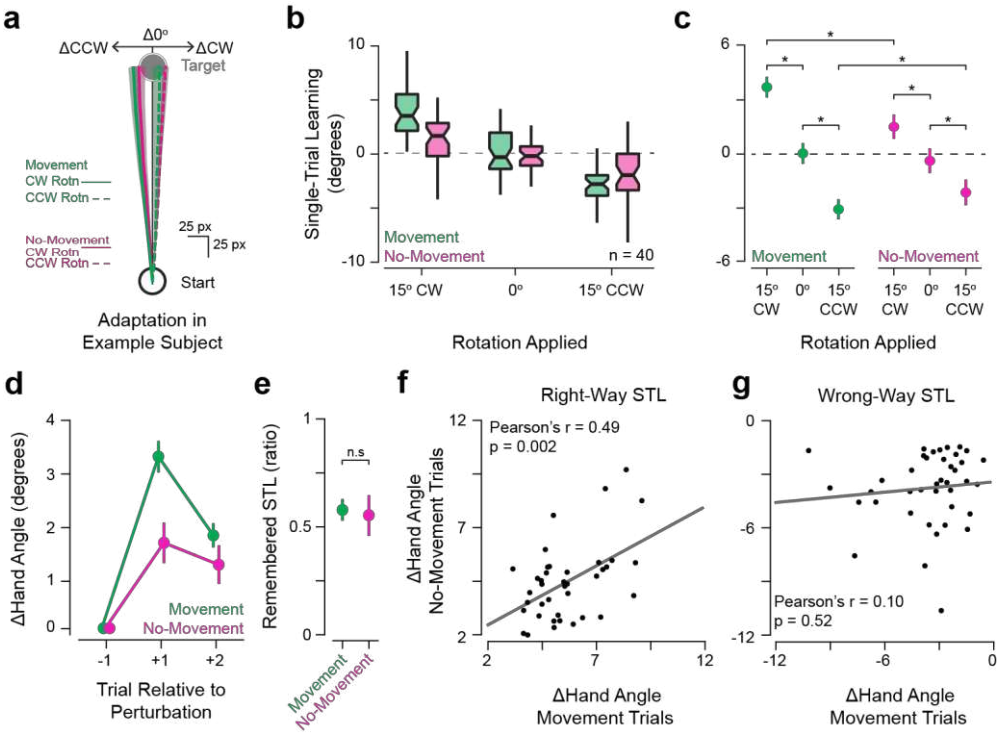

Supplemental Figure 2. Single-trial learning in response to errors on Movement and No-Movement trials during an online visuomotor adaptation task. (**a**) An example participant's mean ± SEM changes in reach paths across triplets (green: triplets with perturbations on Movement trials, magenta: triplets with perturbations on No-Movement trials, solid lines: perturbation was a CW rotation, dashed lines: perturbation was a CCW rotation). (**b**) Boxplot showing STL across Movement (green) and No-Movement (magenta) triplets for participants in an online version of the task described in Figure 1 ($n = 40$). (**c**) Estimated marginal means (EMMs) ± 95% confidence intervals from the linear mixed model (LMM) fit to participants' STL performance (summarized in **b**). The LMM (fixed effects: rotation [15° counterclockwise {CCW}, 0°, and 15° clockwise {CW}], movement condition [Movement, No-Movement], rotation x movement condition interaction; random effects: participant) revealed significant main effects of rotated cursor feedback ($F(2, 2223) = 136.46$, $p = 2.2 \times 10^{-16}$, *partial* $R^2 = 0.11$) and movement condition ($F(1, 2248) = 4.74$, $p = 0.03$, *partial* $R^2 = 0.002$), as well as a significant interaction ($F(2, 2229) = 12.40$, $p = 4.41 \times 10^{-6}$, *partial* $R^2 = 0.01$). Post-hoc pairwise comparisons of the EMMs from the model support the claim that rotated feedback induced a statistically significant degree of STL on both Movement (0° vs 15° CW: $t(2227) = 9.14$, $p_{adj} = 6.39 \times 10^{-19}$, *Cohen's d* = 0.61; 0° vs 15° CCW: $t(2220) = 7.81$, $p_{adj} = 2.61 \times 10^{-14}$, *Cohen's d* = 0.52) and No-Movement trials (0° vs 15° CW: $t(2225) = 3.92$, $p_{adj} = 1.39 \times 10^{-4}$, *Cohen's d* = 0.31; 0° vs 15° CCW: $t(2229) = 3.56$, $p_{adj} = 4.84 \times 10^{-4}$, *Cohen's d* = 0.29). Adaptation in the presence of a rotation was significantly greater in Movement trials than No-Movement trials for CW ($t(2238) = 4.98$, $p_{adj} = 1.26 \times 10^{-6}$, *Cohen's d* = 0.37) and CCW rotations ($t(2239) = 2.06$, $p_{adj} = 0.04$, *Cohen's d* = 0.15). (**d**) Group mean ± SEM change in

(Δ) hand angle after exposure to Movement (green) and No-Movement (magenta) triplets' perturbations. Positive Δ values indicate that the change in hand angle proceeded opposite the direction of the perturbation (*i.e.,* in the direction that would counter the error). (**e**) Group mean ± SEM ratio of remembered STL to STL. Remembered STL was statistically significantly greater than 0 for both Movement (one-sample signed-rank test: $V = 819$, $p_{adj} = 1.09 \times 10^{-11}$, $r = 0.87$) and No-Movement triplets ($V = 769$, $p_{adj} = 9.69 \times 10^{-8}$, $r = 0.76$), but remembered STL did not significantly differ between movement conditions (paired-samples signed-rank test: $V = 441$, $p_{adj} = 0.68$). (**f**) Scatter plot showing the relationship between individual subjects' STL amplitude in the direction opposite the rotation on Movement and No-Movement trials. When we considered instances of STL in the direction that would compensate for the observed error (update opposite rotation, "Right-Way"), within-subject changes in hand angle were correlated between Movement and No-Movement trials (*Pearson's* $r = 0.49$, $p_{adj} = 0.002$). (**g**) As in **f**, but showing data from trials with changes in hand angle in the direction that would exacerbate the observed error (update in direction of rotation, "Wrong-Way"). These ΔHand Angle values were uncorrelated between Movement and No-Movement trials (*Pearson's* $r = 0.10$, $p_{adj} = 0.52$). These observations support the idea that the same learning process may underlie adaptive single-trial learning events in response to errors on both kinds of trials, while maladaptive changes in hand-angle may be attributable to potential sources of random noise. Boxplot centers: median, notch: 95% confidence interval of the median, box edges: 1st and 3rd quartiles, whiskers: most extreme value within 1.5*interquartile range of the median. Statistical significance (* = $p < 0.05$; n.s. = $p \geq 0.05$) is. Abbreviations: STL – single-trial learning, Δ – change, CW – clockwise, CCW – counterclockwise.

Motor adaptation during No-Movement triplets does not depend on participants' control over cursor trajectory during Movement trials

We note that rotated visual feedback on Movement trials was sensitive to people's actual reaching directions. That is, the rotation was simply added to the measured reach direction, as is typical in visuomotor rotation tasks. It is possible that these directional contingencies affected participants' responses to error, potentially encouraging them to attempt to deliberately control the cursor's position via an explicit re-aiming process.[18] To rule this out, we recruited a new group of participants ($n = 37$) to perform a variant of the task where the visual cursor moved in a fixed path ("error-clamped" feedback[17]; **Supplemental Fig. 3**) in one of three directions (0° or 15° CW/CCW) on trials with feedback.

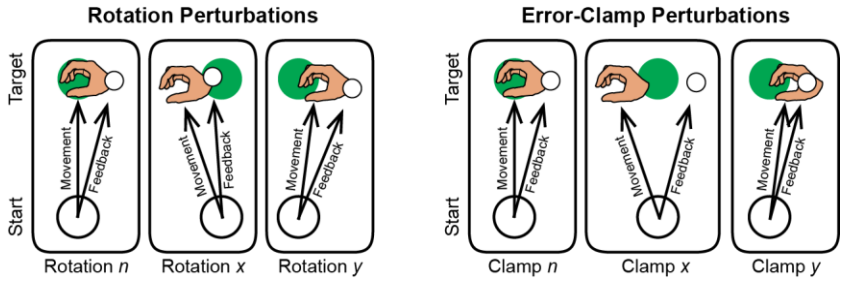

Supplemental Figure 3. Schematics illustrating the difference between rotation and error-clamp perturbations. Diagrams showing the relationship between hand and cursor feedback movement directions under rotational error regimes (left) and error-clamp regimes (right). When rotational

perturbations are applied to cursor feedback, the cursor's movement direction is contingent upon the participant's movement direction, although there is an experimenter-induced offset. If a rotation is consistently applied, participants explicit aiming strategies are a viable supplement for imperfect implicit motor performance. When error-clamp perturbations are applied to cursor feedback, the cursor travels in a fixed direction, regardless of the direction that the hand travels, rendering explicit aiming strategies useless. Thus, error-clamp perturbations are often used in studies attempting to isolate implicit motor adaptation processes.

Replicating and extending the findings from the two studies employing rotated cursor feedback, participants assigned to the error-clamp condition exhibited STL after Movement and No-Movement trials (**Supplemental Fig. 4a-c**; please refer to supplemental material for details). We also observed significant retention of STL (**Supplemental Fig. 4d-e**) and correlation between STL amplitude on Movement and No-Movement trials where adaptation proceeded opposite the direction of the perturbation (**Supplemental Fig. 4f-g**). These data further strengthen the claim that motor adaptation does not require movement.

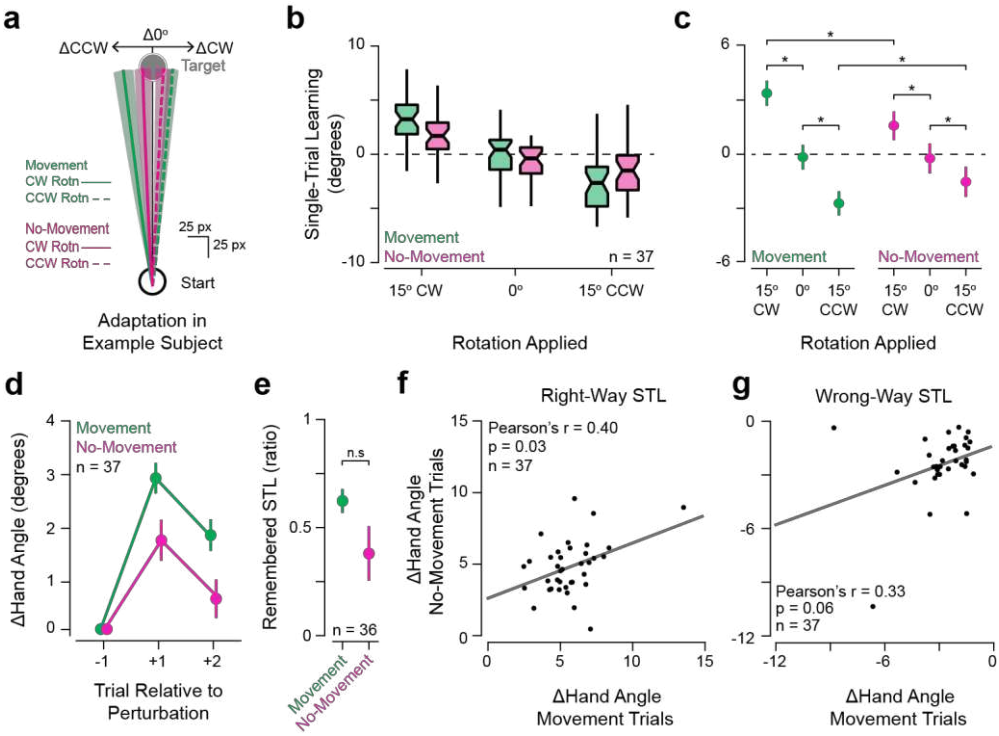

Supplemental Figure 4. Single-trial learning in response to errors on Movement and No-Movement trials with error-clamped feedback or simulated errors. (**a**) An example participant's mean ± SEM changes in reach paths across triplets (green: triplets with perturbations on Movement trials, magenta: triplets with perturbations on No-Movement trials, solid lines: perturbation was a CW error-clamp, dashed lines: perturbation was a CCW error-clamp). (**b**) Boxplot showing STL across Movement (green) and No-Movement (magenta) triplets for participants (n = 37) in an online experiment where cursor feedback was error-clamped on Movement trials. (**c**) Estimated marginal means (EMMs) ± 95% confidence intervals from

the linear mixed model (LMM) fit to participants' STL performance (summarized in **b**). The LMM (fixed effects: rotation [15° counterclockwise {CCW}, 0°, and 15° clockwise {CW}], movement condition [Movement, No-Movement], error-clamp x movement condition interaction; random effects: participant) revealed significant main effects of error-clamped cursor feedback ($F(2, 1829) = 79.46$, $p = 2.2 \times 10^{-16}$, *partial* $R^2 = 0.08$) and an interaction between error-clamp and movement condition ($F(2, 1832) = 8.45$, $p = 0.0002$, *partial* $R^2 = 0.0003$), although there was no main effect of movement condition ($F(1, 1844) = 0.60$, $p = 0.44$). Post-hoc comparisons of the EMMs from the model revealed significant STL in response to non-zero error-clamped feedback on both Movement (0° vs 15° CW: $t(1827) = 7.55$, $p_{adj} = 3.08 \times 10^{-13}$, *Cohen's d* = 0.56; 0° vs 15° CCW: $t(1828) = 5.57$, $p_{adj} = 8.84 \times 10^{-8}$, *Cohen's d* = 0.41) and No-Movement trials (0° vs 15° CW: $t(1830) = 3.21$, $p_{adj} = 0.002$, *Cohen's d* = 0.29; 0° vs 15° CCW: $t(1832) = 2.25$, $p_{adj} = 0.03$, *Cohen's d* = 0.22). Adaptation in the presence of a 15° error-clamp was significantly greater on Movement trials than No-Movement trials for CW ($t(1846) = 3.49$, $p_{adj} = 0.0009$, *Cohen's d* = 0.29) and CCW clamps ($t(1846) = 2.29$, $p_{adj} = 0.03$, *Cohen's d* = 0.19). Please refer to Supplementary Table 2 for further details on post-hoc comparisons in this panel. (**d**) Group mean ± SEM change in (Δ) hand angle one and two trials after exposure to Movement (green) and No-Movement (magenta) triplets' perturbations. Positive Δ values indicate that the change in hand angle proceeded opposite the direction of the perturbation (*i.e.,* in the direction that would counter the error). (**e**) Remembered STL shown as the ratio of relative hand angle 2 trials after experiencing a perturbation to the relative hand angle 1 trial after the perturbation (STL). Remembered STL was significantly greater than 0 after both Movement (green; one-sample t-test: $t(36) = 11.31$, $p_{adj} = 6.23 \times 10^{-13}$, *Cohen's d* = 1.86) and No-Movement triplets (magenta, one-sample signed-rank test: $V = 579$, $p_{adj} = 5.95 \times 10^{-5}$, $r = 0.64$), but did not exhibit statistically significant differences between movement conditions (paired t-test: $t(35) = 1.71$, $p_{adj} = 0.09$). Remembered STL on No-Movement trials could not be computed for one participant, so $n = 36$ instead of 37 in this panel. (**f**) Scatter plot showing the relationship between individual subjects' STL amplitude in the direction opposite the error-clamp on Movement and No-Movement trials (i.e., the "Right-Way"). Right-way changes in hand angle were correlated between Movement and No-Movement trials (*Pearson's* $r = 0.40$, $p_{adj} = 0.03$). (**g**) As in (**f**), but showing data from trials on which STL proceeded in the same direction as the error-clamp (*i.e.*, the "Wrong-Way"). Wrong-Way changes in hand angle were not statistically significantly correlated between Movement and No-Movement trials ($r = 0.33$, $p_{adj} = 0.06$). These observations support the idea that the same learning process may underlie adaptive single-trial learning events in response to errors on both kinds of trials, while maladaptive changes in hand-angle may be attributable to potential sources of random noise. Boxplot centers: median, notch: 95% confidence interval of the median, box edges: 1st and 3rd quartiles, whiskers: most extreme value within 1.5*interquartile range of the median. Statistical significance (* = $p < 0.05$; n.s. = $p \geq 0.05$) is indicated for selected comparisons. Abbreviations: STL – single-trial learning, Δ – change, CW – clockwise, CCW – counterclockwise.

Adaptation on No-Movement trials does not depend on within-session adaptation on Movement trials

In two further experiments, we asked if adaptation to errors in the No-Movement condition was contingent on sharing a context with the Movement condition. In other words, if learning in the No-Movement condition only occurs when there are neighboring trials in the Movement condition producing typical SPEs, it is possible that adaptive responses observed in the No-Movement condition reflect a "cueing" effect, whereby an adapted sensorimotor map is cued by observation of the visual error and then retrieved on the subsequent trial(s). While our previous retention (**Fig. 2d-e**, **Supplemental Fig. 2d-e**,

Supplemental Fig. 4d-e) and correlation (**Fig. 2f-g**, **Supplemental Fig. 2f-g**, **Supplemental Fig. 4f-g**) results argue against this interpretation as they suggest a shared learning mechanism across movement conditions, we opted to directly test this alternative explanation in another pair of experiments. Here, we only included 0° rotated (**Fig. 3a**, left, n = 24 participants) or clamped (**Fig. 3a**, right, n = 37 participants) error feedback on Movement trials, but maintained 0° or 15° CW/CCW errors on the No-Movement trials. The key results were again replicated – learning was preserved in the No-Movement condition even when error feedback had never been associated with executed movements (**Fig. 3c**, rotation: LMM: $F(557)$ 23.01, $p = 2.07 \times 10^{-6}$, *partial* $R^2 = 0.04$; error-clamp: $F(802) = 9.41$, $p = 9.14 \times 10^{-5}$, *partial* $R^2 = 0.02$). Post-hoc pairwise comparisons showed that adaptation was significantly different between triplets with clockwise and counterclockwise errors for both the rotation ($t(557) = 4.80$, $p = 2.07 \times 10^{-6}$, *Cohen's d* = 0.4) and error-clamp experiments ($t(1453) = 4.32$, $p = 5.34 \times 10^{-5}$, *Cohen's d* = 0.37) – a hallmark of implicit motor adaptation (please refer to **Supplemental Table 3** for all post-hoc test results). Overall levels of STL observed on No-Movement trials were comparable during these two experiments to those discussed above, and within the range of learning rates previously observed in the literature (**Supplemental Fig. 1**). Furthermore, both groups of participants showed retention of STL that differed significantly from 0 (rotation, mean ± SEM: 0.53 ± 0.06 retention ratio, one-sample t-test: $t(22) = 8.28$, $p = 3.34 \times 10^{-8}$, *Cohen's d* = 1.73; error-clamp, median: 0.45, interquartile-range: 0.58, one-sample signed-rank test: $V = 507$, $p = 0.001$, $r = 0.53$). Overall, these experiments support our hypothesis that motor adaptation can proceed without movement execution.

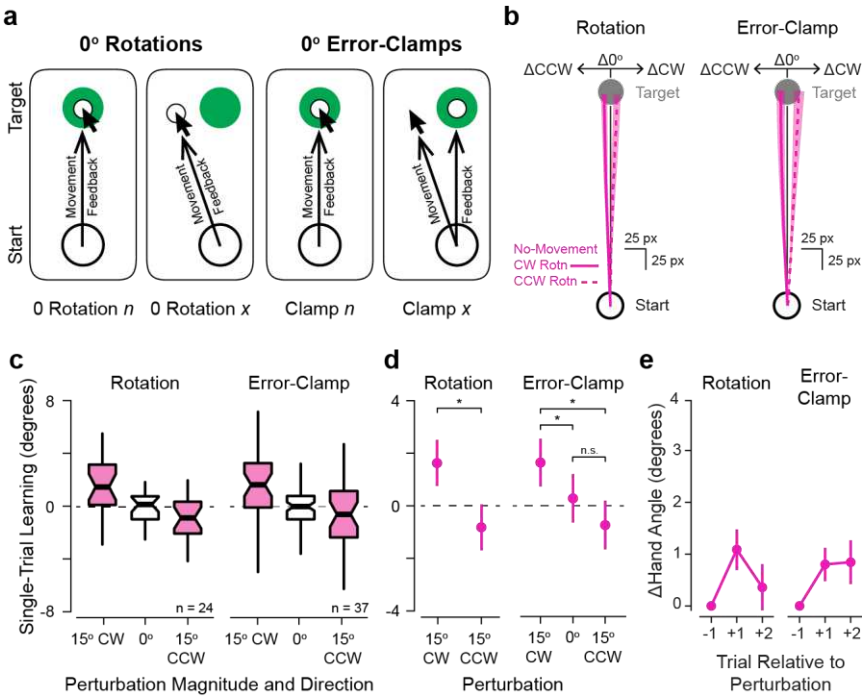

Figure 3. Effects of simulated errors when perturbations were never applied during Movement trials. (**a**) Schematic illustrating the relationship between movement and visual feedback on Movement trials during an experiment where visuomotor rotations (left) or error-clamps (right) were never applied during Movement trials. (**b**) An example participant's mean ± SEM changes in reach paths across No-Movement triplets from studies in which non-zero rotations (left) and error-clamps (right) were never applied (solid lines: perturbation was CW, dashed lines: perturbation was CCW). (**c**) Boxplots showing STL in response to different directions of simulated errors (No-Movement triplets indicated in magenta) from rotation (left, n = 24) and error-clamp (right, n = 37) studies. (**d**) Estimated marginal means ± 95% confidence intervals from the linear mixed models fit to each participant's STL performance summarized in (**c**). Asterisks indicate statistically significant differences. (**e**) Mean ± SEM relative hand angles on the two trials after a perturbation was presented on a No-Movement trial. Please refer to Supplemental Table 3 for detailed statistical results. Boxplot centers: median, notches: 95% confidence interval of the median, box edges: 1st and 3rd quartiles, whiskers: most extreme values within 1.5*IQR of the median. Statistical significance (* = $p_{adj} < 0.05$; n.s. = $p_{adj} \geq 0.05$) is indicated for selected comparisons. Abbreviations: STL – single-trial learning, CW – clockwise, CCW – counterclockwise, Δ – change in.

DISCUSSION

The results presented above demonstrate that movements can be implicitly refined even when they are not performed. Participants who were cued to perform a movement towards a target but suppressed that movement after observation of a Stop cue showed consistent, robust STL in response to simulated errors (**Figs. 2-3**, **Supplemental Fig. 2**, **Supplemental Fig. 4**). As implicit learning necessarily proceeds following SPEs, our data also provide evidence that SPEs are computed even when movements are not performed. These findings strongly support the fundamental assumptions of predictive processing

397 frameworks of motor adaptation, where precise sensory predictions are generated from a movement intent
398 (or "plan", "goal") and compared against sensory observations to induce error-based learning.[12,25]
399 We argue that we have measured learning via an implicit process, and, by extension, that the STL
400 observed in our study provides evidence that SPEs are computed regardless of whether a movement is
401 performed. Although it is important to note that visuomotor learning tasks do sometimes recruit cognitive
402 learning strategies (e.g., the deliberate "re-aiming" of movements), multiple factors indicate that our studies
403 successfully measured implicit adaptation.[18,28,29] First, in line with previous work isolating the implicit
404 adaptation process, participants were instructed to ignore the visually displayed cursor and try to contact
405 the target on every trial, a straightforward technique which has been consistently shown to eliminate the
406 explicit re-aiming of movements.[15,17,22,23,26] Second, the randomization of both the presence and direction
407 of visual errors also discourages explicit learning, reducing motivation to apply ineffective re-aiming
408 strategies (see [30]). Third, we excluded data from participants who did not understand or recall the instruction
409 to always aim directly at the target (see *Methods*), decreasing the likelihood that strategic re-aiming
410 contaminated the analysis. Fourth, adaptation persisted into subsequent no-feedback trials (**Fig. 2d-e**, **Fig.**
411 **3e**, **Supplemental Fig. 2d-e**, **Supplemental Fig. 4d-e**), a finding that is consistent with lingering implicit
412 motor learning; it is unlikely that strategies would be maintained through trials where no feedback is present.
413 Fifth, the magnitude of STL observed was consistent with multiple previous studies that measured implicit
414 motor adaptation rates (**Supplemental Fig. 1**).[17,23,31] Lastly, the adaptation effects observed in the No-
415 Movement conditions were not attributable to recall of learning that occurred on Movement trials (**Fig. 3**.
416 Our data thus provide striking evidence that movement is not required for implicit adaptation, and, by
417 extension, SPE computation.
418 While motor planning and concurrent sensory observations are sufficient to drive SPE computation
419 and motor adaptation, our data also indicate that errors paired with movements support a greater degree
420 of learning than errors without preceding movements, as participants showed significantly stronger STL
421 over triplets with Movement trials versus No-Movement trials. This suggests that movement provides
422 additional training input beyond what erroneous visual feedback provides alone. Alternately (though not
423 mutually exclusive), it may be that the absence of movement-related proprioceptive feedback dampens the
424 SPE signals that drive adaptation, perhaps by failing to counterbalance signals predicting proprioceptive

425 feedback.[8,32] Simpler explanations are that participants simply did not recognize the Go cue to set a
426 movement goal and plan a movement on a subset of the No-Movement trials, and/or that the timing of the
427 simulated error was inherently too variable relative to the behaviorally unobservable internal prediction.
428 Further experimentation will be required to address these possibilities. Nonetheless, our data demonstrate
429 the significant influence of the brain's prediction signals on learning – even without the ability to directly
430 attribute sensory feedback to an actual movement, prediction of a planned movement's sensory
431 consequences supports the error computations that drive adaptation of future behavior.

432 While our results demonstrate that overt movement is not necessary for motor adaptation, we are
433 not able to discern whether the generation of a descending motor command is a necessary component for
434 updating the forward model. To reliably elicit prediction generation from the forward model, we employed a
435 motor inhibition paradigm, briefly cueing participants to reach before presenting them with an abrupt stop
436 signal. This strategy is likely to have recruited mechanisms of motor inhibition beyond the primary motor
437 cortex, leaving open the possibility that a descending motor command and not an upstream motor plan *per*
438 *se* provide the necessary input for forward model adaptation.[33–35] Future experimentation quantifying neural
439 (EEG) or physiological (EMG) signals during this task and measuring their relationship with adaptation on
440 No-Movement trials will be crucial for addressing this point. Inspired by work in non-human primates, we
441 speculate that similar motor cortical preparatory states in the Movement and No-Movement conditions may
442 produce comparable inputs to downstream internal models.[36]

443 The current report provides evidence that implicit motor adaptation can proceed without movement,
444 adding to a substantial body of work indicating that many forms of motor learning do not strictly require
445 movement-based practice. For instance, in [35], after human participants observed others adapting to a force
446 field applied during reaching movements, the observers were able to partially compensate for that same
447 force field when they encountered it. Interestingly, this observational learning did not proceed if participants
448 were executing other movements during the observation period. This finding combined with subsequent
449 neuroimaging data showing that observational learning recruits brain areas associated with motor planning
450 were taken to suggest that engagement in a covert motor planning process may be the critical element
451 allowing for force-field adaptation following error observation without movement.[37–39] Together, this related
452 prior work and the evidence we have provided that motor planning is sufficient for the generation of sensory

predictions and can support SPE computations suggest that there are multiple routes to inducing motor planning and ultimately driving motor adaptation processes.

Other reports in the motor learning literature have provided evidence for cognitive compensation for observed motor errors during reaching, improved visual tracking following observation of target movement without engagement in visual pursuit, and improvement in movement speeds as a result of mental imagery training, highlighting the breadth of motor performance-related processes that can be trained without engagement in physical movements.[19,20,40,41] Together with the findings related to implicit motor adaptation discussed above, this work suggests that many features of motor performance can be improved by training regiments that do not involve movement. This work points to a potential opportunity for the development of motor training or rehabilitation protocols that can be used when people are unable to physically perform target motor behaviors, perhaps improving performance beyond what physical practice can do alone.

Finally, our results echo the fact that other types of learning also appear to occur without overt task execution. Outside of motor learning, fear associations can be extinguished by instructing participants to imagine a fear-predicting stimulus even when they are not presented with the stimulus, with this “imagination” protocol generating neural signatures of the negative prediction errors observed during naturalistic fear extinction.[42,43] Considering this prior work and the findings presented in this study, it may be that the generation of predictions for comparison with subsequent sensory observations is sufficient for error-based learning across motor and non-motor domains alike. In other words, task execution may not always be required for learning, so long as the predictions and observations needed to compute errors are both present.

REFERENCES

1. Friston, K. The free-energy principle: a unified brain theory? *Nat Rev Neurosci* **11**, 127–138 (2010). doi: 10.1038/nrn2787
2. Jordan, M. I. & Rumelhart, D. E. Forward models: Supervised learning with a distal teacher. *Cognitive Science* **16**, 307–354 (1992). doi: 10.1016/0364-0213(92)90036-T
3. Wallman, J. & Fuchs, A. F. Saccadic gain modification: Visual error drives motor adaptation. *Journal of Neurophysiology* **80**, 2405–2416 (1998). doi: 10.1152/jn.1998.80.5.2405
4. Shadmehr, R., Smith, M. A. & Krakauer, J. W. Error correction, sensory prediction, and adaptation in motor control. *Annu. Rev. Neurosci.* **33**, 89–108 (2010). doi:10.1146/annurev-neuro-060909-153135
5. Tseng, Y., Diedrichsen, J., Krakauer, J. W., Shadmehr, R. & Bastian, A. J. Sensory prediction errors drive cerebellum-dependent adaptation of reaching. *Journal of Neurophysiology* **98**, 54–62 (2007). doi: 10.1152/jn.00266.2007
6. Wong, A. L. & Shelhamer, M. Sensorimotor adaptation error signals are derived from realistic predictions of movement outcomes. *Journal of Neurophysiology* **105**, 1130-1140 (2011). doi: 10.1152/jn.00394.2010
7. Held, R. & Freedman, S. J. Plasticity in human sensorimotor control. *Science* **142**, 455–462 (1963).
8. Miall, R. C. & Wolpert, D. M. Forward Models for Physiological Motor Control. *Neural Networks* **9**, 1265–1279 (1996). doi: 10.1016/S0893-6080(96)00035-4
9. Kilteni, K., Andersson, B. J., Houborg, C. & Ehrsson, H. H. Motor imagery involves predicting the sensory consequences of the imagined movement. *Nat Commun* **9**, 1617 (2018). doi: 10.1038/s41467-018-03989-0
10. Voss, M., Ingram, J. N., Haggard, P. & Wolpert, D. M. Sensorimotor attenuation by central motor command signals in the absence of movement. *Nat Neurosci* **9**, 26–27 (2006). doi: 10.1038/nn1592
11. Sheahan, H. R., Franklin, D. W. & Wolpert, D. M. Motor Planning, Not Execution, Separates Motor Memories. *Neuron* **92**, 773–779 (2016). doi: 10.1016/j.neuron.2016.10.017
12. Sheahan, H. R., Ingram, J. N., Žalalytė, G. M. & Wolpert, D. M. Imagery of movements immediately following performance allows learning of motor skills that interfere. *Sci Rep* **8**, 14330 (2018). doi: 10.1038/s41598-018-32606-9
13. Butcher, P. A. & Taylor, J. A. Decomposition of a sensory prediction error signal for visuomotor adaptation. *Journal of Experimental Psychology: Human Perception and Performance* **44**, 176–194 (2018). doi: 10.1037/xhp0000440
14. Tsay, J. S., Haith, A. M., Ivry, R. B. & Kim, H. E. *Interactions between sensory prediction error and task error during implicit motor learning*. 2021.06.20.449180 https://www.biorxiv.org/content/10.1101/2021.06.20.449180v2 (2021) doi:10.1101/2021.06.20.449180.
15. McDougle, S. D., Ivry, R. B. & Taylor, J. A. Taking aim at the cognitive side of learning in sensorimotor adaptation tasks. *Trends in Cognitive Sciences* **20**, 535–544 (2016). doi: 10.1016/j.tics.2016.05.002
16. Mazzoni, P. & Krakauer, J. W. An implicit plan overrides an explicit strategy during visuomotor adaptation. *J. Neurosci.* **26**, 3642–3645 (2006). doi: 10.1523/JNEUROSCI.5317-05.2006
17. Morehead, J. R., Taylor, J. A., Parvin, D. E. & Ivry, R. B. Characteristics of implicit sensorimotor adaptation revealed by task-irrelevant clamped feedback. *J Cogn Neurosci* **29**, 1061–1074 (2017). doi: 10.1162/jocn_a_01108
18. Taylor, J. A., Krakauer, J. W. & Ivry, R. B. Explicit and implicit contributions to learning in a sensorimotor adaptation task. *The Journal of Neuroscience* **34**, (2014).
19. Ong, N. T. & Hodges, N. J. Absence of after-effects for observers after watching a visuomotor adaptation. *Exp Brain Res* **205**, 325–334 (2010). doi: 10.1007/s00221-010-2366-4

20. Lim, S. B., Larssen, B. C. & Hodges, N. J. Manipulating visual–motor experience to probe for observation-induced after-effects in adaptation learning. *Exp Brain Res* **232**, 789–802 (2014). doi: 10.1007/s00221-013-3788-6
21. Taylor, J. A. & Ivry, R. B. Flexible cognitive strategies during motor learning. *PLOS Computational Biology* **7**, e1001096 (2011). doi: 10.1371/journal.pcbi.1001096
22. Tsay, J. S., Parvin, D. E. & Ivry, R. B. Continuous reports of sensed hand position during sensorimotor adaptation. *Journal of Neurophysiology* **124**, 1122–1130 (2020). doi: 10.1152/jn.00242.2020
23. Kim, H. E., Morehead, J. R., Parvin, D. E., Moazzezi, R. & Ivry, R. B. Invariant errors reveal limitations in motor correction rather than constraints on error sensitivity. *Communications Biology* **1**, 1–7 (2018). doi: 10.1038/s42003-018-0021-y
24. Avraham, G., Morehead, J. R., Kim, H. E. & Ivry, R. B. Reexposure to a sensorimotor perturbation produces opposite effects on explicit and implicit learning processes. *PLOS Biology* **19**, e3001147 (2021). doi: 10.1371/journal.pbio.3001147
25. Poh, E., Al-Fawakari, N., Tam, R., Taylor, J. A. & McDougle, S. D. Generalization of motor learning in psychological space. *bioRxiv* 2021.02.09.430542 (2021) doi:10.1101/2021.02.09.430542. doi: 10.1101/2021.02.09.430542
26. Hadjiosif, A. M., Krakauer, J. W. & Haith, A. M. Did we get sensorimotor adaptation wrong? Implicit adaptation as direct policy updating rather than forward-model-based learning. *J. Neurosci.* **41**, 2747–2761 (2021). doi: 10.1523/JNEUROSCI.2125-20.2021
27. Wei, K. & Körding, K. Relevance of error: What drives motor adaptation? *Journal of Neurophysiology* **101**, 655–664 (2009). doi: 10.1152/jn.90545.2008
28. Krakauer, J., W., Hadjiosif, A., Xu, J. & Wong, A., L. Motor Learning. in *Comprehensive Physiology* (ed. Terjung, R.) (Wiley, 2019). doi:10.1002/cphy.
29. McDougle, S. D. & Taylor, J. A. Dissociable cognitive strategies for sensorimotor learning. *Nat Commun* **10**, 40 (2019). doi: 10.1038/s41467-018-07941-0
30. Hutter, S. A. & Taylor, J. A. Relative sensitivity of explicit reaiming and implicit motor adaptation. *Journal of Neurophysiology* **120**, 2640–2648 (2018). doi: 10.1152/jn.00283.2018
31. Wei, K. & Körding, K. Uncertainty of feedback and state estimation determines the speed of motor adaptation. *Front. Comput. Neurosci.* **4**, (2010). doi: 10.3389/fncom.2010.00011
32. Requarth, T., Kaifosh, P. & Sawtell, N. B. A role for mixed corollary discharge and proprioceptive signals in predicting the sensory consequences of movements. *J. Neurosci.* **34**, 16103–16116 (2014). doi: 10.1523/JNEUROSCI.2751-14.2014
33. Xu, K. Z., Abderson, B. A., Emeric, E .E., Sali, A. W., Stuphorn, V., Yantis, S., Courtney, S. M. Neural basis of cognitive control over movement inhibition: Human fMRI and primate electrophysiology evidence. *Neuron* **96**, 1447-1458.e6 (2017). doi: 10.1016/j.neuron.2017.11.010
34. Osada, T., Ohta, S., Ogawa, A., Tanaka, M., Suda, A., Kamagata, K., Hori, M., Shigeki, A., Shimo, Y., Hattori, N., Shimizu, T., Enomoto, H., Hanajima, R., Ugawa, Y., Konishi, S. An essential role of the intraparietal sulcus in response inhibition predicted by parcellation-based network. *J. Neurosci.* **39**, 2509–2521 (2019). doi: 10.1523/JNEUROSCI.2244-18.2019
35. Duque, J., Greenhouse, I., Labruna, L. & Ivry, R. B. Physiological Markers of Motor Inhibition during Human Behavior. *Trends in Neurosciences* **40**, 219–236 (2017). doi: 10.1016/j.tins.2017.02.006
36. Vyas, S, Even-Chen, N., Stavitsky, S. D., Ryu, S. I., Nuyujukian, P., Shenoy, K. V. Neural population dynamics underlying motor learning transfer. *Neuron* **97**, 1177-1186.e3 (2018). doi: 10.1016/j.neuron.2018.01.040
37. Mattar, A. A. G. & Gribble, P. L. Motor Learning by Observing. *Neuron* **46**, 153–160 (2005). doi: 10.1016/j.neuron.2005.02.009

38. Malfait, N., Valyear, K. F., Culham, J. C., Anton, J., Brown, L. E., Gribble, P. L. fMRI activation during observation of others' reach errors. *Journal of Cognitive Neuroscience* **22**, 1493–1503 (2010). doi: 10.1162/jocn.2009.21281
39. McGregor, H. R. & Gribble, P. L. Functional connectivity between somatosensory and motor brain areas predicts individual differences in motor learning by observing. *Journal of Neurophysiology* **118**, 1235–1243 (2017). doi: 10.1016/j.cub.2016.01.064
40. Gentili, R., Han, C. E., Schweighofer, N. & Papaxanthis, C. Motor Learning Without Doing: Trial-by-Trial Improvement in Motor Performance During Mental Training. *Journal of Neurophysiology* **104**, (2010).
41. Cain, M., Botschko, Y. & Joshua, M. Passive motor learning: Oculomotor adaptation in the absence of behavioral errors. *eNeuro* **8**, (2021). doi: 10.1523/ENEURO.0232-20.2020
42. Mendelsohn, A., Pine, A. & Schiller, D. Between thoughts and actions: Motivationally salient cues invigorate mental action in the human brain. *Neuron* **81**, 207–217 (2014). doi: 10.1016/j.neuron.2013.10.019
43. Reddan, M. C., Wager, T. D. & Schiller, D. Attenuating neural threat expression with imagination. *Neuron* **100**, 994-1005.e4 (2018). doi: 10.1016/j.neuron.2018.10.047
44. Herzfeld, D. J., Vaswani, P. A., Marko, M. K. & Shadmehr, R. A memory of errors in sensorimotor learning. *Science* **345**, 1349–1353 (2014). doi: 10.1126/science.1253138
45. van Beers, R. J. Motor learning Is optimally tuned to the properties of motor noise. *Neuron* **63**, 406–417 (2009). doi: 10.1016/j.neuron.2009.06.025
46. Wu, H. G., Miyamoto, Y. R., Castro, L. N. G., Ölveczky, B. P. & Smith, M. A. Temporal structure of motor variability is dynamically regulated and predicts motor learning ability. *Nat Neurosci* **17**, 312–321 (2014). doi: 10.1038/nn.3616
47. Photon Storm. Phaser (V. 3.24.1). https://phaser.io (2020).
48. Tsay, J. S., Ivry, R. B., Lee, A. & Avraham, G. Moving outside the lab: The viability of conducting sensorimotor learning studies online. *NBDT* 1–22 (2021) doi:10.51628/001c.26985.
49. Kassambara, A. *rstatix: Pipe-Friendly Framework for Basic Statistical Tests*. (2021).
50. Hothorn, T., Hornik, K., van de Wiel, M. A. & Zeileis, A. Implementing a class of permutation tests: The coin package. *Journal of Statistical Software* **28**, 1–23 (2008). doi: 10.18637/jss.v028.i08
51. Bartoń, K. *MuMIn: Multi-Model Inference*. (2020).
52. Kuznetsova, A., Brockhoff, P. B. & Christensen, R. H. B. lmerTest package: Tests in linear mixed effects models. *Journal of Statistical Software* **82**, 1–26 (2017). doi: 10.18637/jss.v082.i13
53. Bates, D., Mächler, M., Bolker, B. & Walker, S. Fitting linear mixed-effects models using lme4. *arXiv:1406.5823 [stat]* (2014).
54. Jaeger, B. *r2glmm: Computes R Squared for Mixed (Multilevel) Models*. (2017).
55. Lenth, R. V. *emmeans: Estimated Marginal Means, aka Least-Squares Means*. (2021).
56. Torchiano, M. *effsize: Efficient Effect Size Computation*. (2020).
57. Ben-Shachar, M., Lüdecke, D. & Makowski, D. effectsize: Estimation of effect size indices and standardized parameters. *Journal of Open Source Software* **5**, 7 (2020). doi: 10.21105/joss.02815
58. Bache, S. M., Wickham, H. & RStudio. *magrittr: A Forward-Pipe Operator for R*. (2020).
59. Wickham, H. *ggplot2: Elegant Graphics for Data Analysis*. (Springer-Verlag, 2016).
60. Kassambara, A. *ggpubr: 'ggplot2' Based Publication Ready Plots*. (2020).
61. Lüdecke, D. ggeffects: Tidy Data Frames of Marginal Effects from Regression Models. *JOSS* **3**, 772 (2018). doi: 10.21105/joss.00772

METHODS

Participants. Participants (*n* = 233, aged 18-35, 126 female) recruited from the research participation pools at Princeton/Yale University and on Prolific provided informed consent, approved by each University's IRB. Seventy-five participants were excluded (10 from the dataset collected for Supplemental Fig. 2, 13 from the dataset collected for Supplemental Fig. 4, 26 from the dataset collected for the rotation perturbation experiments described in Fig. 3, and 26 from the dataset collected for the error-clamp perturbation experiments described in Fig. 3) for failure to sufficiently recall task instructions, as ascertained by a questionnaire at the end of the experiment, leaving 158 participants for our analyses. See the *Questionnaire* section below the *Test phase* sections for more details. We note that all the key results described here (*i.e.,* statistically significant learning after No-Movement trials) held with or without these exclusions; we opted to be conservative in our exclusion criteria to limit potential effects of explicit learning. We note that the samples used for the online experiments described in the text are around twice the size of similar studies in the literature, providing additional statistical power to compensate for the experiment being conducted remotely.[44–46]

Task Setup: In Lab. Participants were seated in a chair and made ballistic reaching movements while grasping the handle of a robotic manipulandum with their dominant hand (Kinarm End-Point). The manipulandum restricted movements to the horizontal plane. All visual stimuli were projected to the participant via a horizontal display screen (60 Hz) reflected onto a semi-silvered mirror mounted above the robotic handle. The mirror occluded vision of the arm, hand, and robotic handle, preventing direct visual feedback of hand position. Tasks were programmed in Matlab 2019a's Simulink for deployment in Kinarm's Dexterit-E software (version 3.9). Movement kinematics were recorded at 1 kHz. Each participant viewed a single target located at either 45°, 135°, 225°, or 315° (with target position counterbalanced across participants), 8 cm from a central starting location. The target was visible throughout the experiment.

Task Setup: Online. Experiments were conducted remotely using a custom JavaScript web application based on Phaser 3.24 (download available at [47]), similar to an approach previously described.[48] Each participant viewed a single target located at either 45°, 135°, 225°, or 315° (with target position

640 counterbalanced across participants), 250 pixels from a central starting location. The target was visible
641 throughout the experiment.

642 Participants used an input device of their choice to control their computer cursor during center-out
643 movements. One participant reported using a touchscreen device and was excluded from all analyses. The
644 remaining participants reported using either a trackpad (n = 112), an optical mouse (n = 86), or a trackball
645 (n = 14). A linear mixed model (LMM) did not show effects of Mouse Type on single-trial learning (STL),
646 although we observed that participants using a trackpad exhibited longer reaction times than others,
647 consistent with a previous report.[48]

648 Mouse position sampling rates depended on the exact hardware that each participant used to
649 complete the task. Sampling rates were likely affected by features of the specific mouse used, along with
650 features of the specific computer used, as computers may limit the rate at which the browser samples data
651 in order to cope with limited processing power. In general, sampling rates were around 60 Hz (median ±
652 interquartile range across all 213 online participants recruited: 62.46 ± 2.17 Hz) but ranged from 19.23 Hz
653 to 249.69 Hz. Note that the vast majority of sampling rates were near 60 Hz: Only 5% of sampling rates
654 were < 41.79 Hz, and only 5% of sampling rates were > 126.65 Hz.

655

656 *Baseline training phase.* For in-lab participants, the robot moved the participant's hand to a central starting
657 location (depicted by a grey circle) at the middle of the display while hand and cursor feedback were hidden.
658 They were instructed to hold their hand still in the starting location util the target turned green, at which
659 point they should make a straight slicing movement through the target. After a 100 ms delay, the robot
660 moved the hand back to the starting location. Participants completed 5 of these trials with online and
661 endpoint cursor feedback, followed by 5 trials without visual feedback of the cursor location. Endpoint
662 feedback was constituted by the cursor remaining at the position where it had passed the target radius for
663 50 ms. Participants then completed 10 alternating trials on which the target turned green and stayed green
664 (Execution, 'Go' trials) and on which the target turned magenta 100 ms after turning green, signaling that
665 participants should withhold their movement (No-Movement, 'Stop' trials). After this baseline phase,
666 participants were instructed to continue following these instructions for the remainder of the experiment.

667 Online participants experienced an identical baseline phase, with the exception that they were
668 instructed to move their mouse into a central starting location on the first trial and subsequently saw their
669 mouse cursor reappear near the starting location 100 ms after the completion of the reaching movement,
670 so that participants could quickly return to the start location to initiate the next trial.
671
672 *Test phase: Rotation and Error-Clamp Experiments (Fig. 2, Supplemental Fig. 2, Supplemental Fig. 4).*
673 During the test phase, 480 (in-lab) or 270 (online) total trials were divided into 3-trial triplets (**Fig. 1c**). The
674 first and last trials of all triplets were Go trials, and participants received neither online nor endpoint feedback
675 about cursor location on these trials. The second trial of each triplet was either a Movement or a No-
676 Movement trial. On Movement trials, participants either received rotated/error-clamped[17] visual feedback
677 (15° clockwise [-, CW] or counterclockwise [+, CCW], with sign randomized across trials) or veridical/0°
678 error-clamped visual feedback of their cursor location. On No-Movement (Stop) perturbation trials,
679 participants viewed a brief animation of the cursor moving straight to the center of the target following a
680 trajectory deflected by ±15° from the target center. Animation onset latency was set as a running median
681 of the participant's reaction times on the previous 5 trials. Animation duration was set as a running median
682 of the participant's movement times on the previous 5 trials. If a participant took longer than 400 ms to
683 execute a movement, 800 ms to initiate the movement, their reach trajectory changed by >10° during the
684 movement, or the reach terminated ≥ 60° away from the target, they received a warning and a 4s time-out.
685 If a participant moved their hand (>5 mm in-lab [radius of the starting location]; anything >0 pixels online)
686 on a No-Movement trial, the trial was immediately aborted, and they received a warning and a 4s time-out.
687 The Stop manipulation was successful: Across the experiments, participants erroneously moved on 34.39
688 ± 20.63% (mean ± standard deviation) of Stop trials, suggesting that, for the most part, they were
689 consistently planning movements on Stop trials.
690 For in-lab studies, we used 4 possible triplet perturbation trial types (Movement/No-Movement:
691 ±15°), each of which occurred 40 times throughout each session. For online studies, we used 6 possible
692 triplet perturbation trial types (Movement/No-Movement: ±15° or 0°), each of which occurred 15 times
693 throughout each session. Triplets were pseudorandomly presented within each block, with the constraints
694 that a single rotation (±15° or 0°) could not occur on more than 2 consecutive triplets and that the same

movement condition (i.e., Movement or No-Movement) could not occur on more than 3 consecutive triplets. Three repetitions of each triplet type occurred in blocks of 18 triplets, and participants received a break after each of these blocks.

Test phase: Rotation and Error-Clamp Experiments with 0° Perturbations on Movement Trials (Fig. 3). Experiments were conducted as described above for the other online experiments, with the exception of the details described in this section. For the experiments described in **Fig. 3a-d**, we used a reduced set of 3 possible triplet Perturbation trial types (No-Movement, 15° clockwise error; No-Movement, 15° counterclockwise error; Movement, 0° rotation). We maintained an equal number of Movement and No-Movement triplets throughout the session in order to ensure that participants would reliably respond to the "Go" cue presented at the start of each trial. So, each No-Movement triplet type occurred 22 times, while the Movement triplet type occurred 44 times. Triplets were pseudorandomly presented within each block, with the constraints that a single non-zero rotation (15° clockwise, 15° counterclockwise) could not occur on more than 2 consecutive triplets.

For the experiments described in **Fig. 3e-h**, we used a set of 4 possible triplet Perturbation trial types (No-Movement, 15° clockwise error; No-Movement, 15° counterclockwise error; No-Movement, 0° error; Movement, 0° error-clamp). To maintain an equal number of Movement and No-Movement triplets throughout the session, each No-Movement triplet type occurred 15 times and the Movement triplet type occurred 45 times.

Questionnaire: As we could not receive verbal confirmation that participants understood the task instructions in the online version of the task, we asked subjects to fill out a brief questionnaire to query their understanding of the task. The questionnaire asked participants to attest whether or not 1) their goal was to move the real mouse and not the cursor straight through the green targets and whether or not 2) their goal was to move the white cursor (not the real mouse) straight through the green targets. Participants could select the options, "True," "False," or "Not Sure." Participants were considered to have understood the instructions if they answered both questions correctly (i.e., answered "True" to question 1 and "False" to question 2). The majority of participants answered both questions correctly (138 of 213 participants

723 [65%]), suggesting that most participants understood the task instructions. Nonetheless, these participants
724 made up the dataset for all reported analyses for the online experiments, and all other online participants
725 were excluded from analyses to exclude potential effects of explicit re-aiming.
726
727 *Data analysis.* Data were processed in Python 3.8.5 and Matlab 2018a. Trials with movement were
728 excluded from analysis 1) if any of the reaches in the triplet were not straight (aspect ratio > participant-
729 wise mean + 3 * participant-wise standard deviation), 2) if the participant received any warning for failure
730 to follow task instructions (see *Feedback for failure to follow task instructions*, above), or 3) if the triplet
731 included a No-Movement No-Go perturbation trial with any detectable mouse movement (>0 pixels online,
732 >5 mm in lab).
733 Reach endpoint angle was computed as the angular distance between the center of the target and
734 the point at which the mouse passed the target's radial distance. Because mouse sampling rates did not
735 always allow us to measure mouse position at the exact target radius during the online study, we used the
736 last sample before and the first sample after the mouse passed the target radius to compute an interpolated
737 mouse position at the target radius, as described in a previous report.[48] We note that analyses comparing
738 these measures to measurements at the last sample of the reach (even when it was beyond the target) or
739 the hand angle at peak velocity did not result in substantially different hand angle measurements or
740 statistical outcomes.
741 Single-trial learning (STL) was measured as the difference between reach endpoint angle on the
742 third and first trial of each triplet. For our initial analyses, the sign of STL corresponded to the direction of
743 the relative change in hand angle, with clockwise changes in hand angle taking a negative sign and
744 counterclockwise changes in hand angle taking a positive sign. When we collapsed STL data across
745 rotation directions, we normalized the sign of STL so that changes in hand angle opposite the direction of
746 the imposed rotation took a positive sign and changes in the direction of the rotation took a negative sign.
747 Remembered STL was quantified as the difference between reach endpoint angle on the first trial
748 of one triplet and reach endpoint angle on the first trial of the previous triplet. When remembered STL is
749 reported as a ratio, this value was computed by dividing remembered STL by the STL attributable to a given
750 triplet.

Statistics. Statistical tests were conducted in R (v. 4.0.3; packages rstatix[49], coin[50], MuMIn[51], lmerTest[52], lme4[53], r2glmm[54], emmeans[55], effsize[56], effectsize[57], magrittr[58], ggplot2[59], ggpubr[60], ggeffects[61]). Data from in-lab experiments were analyzed using a two-way repeated measures ANOVA. If an ANOVA showed a significant main effect or interaction, post-hoc pairwise tests were performed. When samples failed to satisfy the normality assumption of the pairwise t-test (assessed via a Shapiro-Wilk test), we used the more robust paired-samples Wilcoxon signed-rank test. Otherwise, we used the more powerful paired t-test. Effect sizes for ANOVA main effects/interactions were quantified via generalized η^2 (η_G^2), we quantified the effect sizes for t-tests using Cohen's d, and we used the Wilcoxon effect size (r) to quantify effect sizes for signed-rank tests. For these and all subsequent analyses, we corrected for multiple comparisons using the false-discovery rate approach to maintain family-wise alpha at 0.05.

Data from the experiments conducted online did not satisfy multiple assumptions of the two-way repeated measures ANOVA (non-existence of extreme outliers, sphericity), so we employed a linear mixed modeling (LMM; R package lmerTest and lme4) approach for analysis of these data. All LMM's included fixed effects of perturbation size and movement condition, as well as random effects of subject. Degrees of freedom were estimated using the Kenward-Rogers approach, and LMM outcomes were reported using ANOVA-style statistics. Partial R^2 was computed to report effect sizes for the LMM factors (R package r2glmm). Post-hoc pairwise comparisons were performed between estimated marginal means computed from the LMM (R package emmeans).

For one-off comparisons between samples or to distributions with 0-mean, we checked samples for normality. When samples were normally distributed, we ran t-tests and computed Cohen's d to report effect sizes for statistically significant results. Otherwise, we ran Wilcoxon-signed rank tests and measured effect sizes using the Wilcoxon effect size (r).

774 **FIGURE LEGENDS**

775 **Figure 1. Schematics showing the proposed learning framework and task design.** (**a**) Schematic
776 showing how the forward model may support implicit motor adaptation in the presence of sensory feedback
777 not causally related to self-generated movement. (**b**) Schematic of events on trials with visual feedback.
778 The robotic apparatus brought the participant's hand to the starting location to initiate a trial. On Movement
779 trials (top), the target turned green ('GO'), cueing participants to reach through the target. On trials with
780 visual feedback, participants observed a white feedback cursor move along a rotated trajectory ('Rotation').
781 On No-Movement trials (bottom), the target turned magenta 100 ms after turning green, cueing participants
782 to withhold movement ('STOP'). After a delay, an animation showing the feedback cursor moving 15° off-
783 target played ('Animation'). The hand is shown in the figure for illustrative purposes but was not visible
784 during the experiment. (**c**) Schematic showing the trials that constituted a triplet and how single-trial learning
785 (STL) was computed. Triplets were composed of 2 Movement trials without visual feedback flanking either
786 a Movement or a No-Movement trial with visual feedback. STL was measured as the difference between
787 reach angles on the flanking trials. (**d**) Schematic showing the pseudorandomized order in which trials were
788 presented for an example participant, with color reflecting the movement condition (Movement: green, No-
789 Movement: magenta).

790

791 **Figure 2. Effects of typical and simulated errors during a visuomotor reach adaptation task.** (**a**)
792 Schematic illustrating how STL and remembered STL measurements were computed. (**b**) An example
793 subject's (top) and the group's (bottom) mean ± SEM changes in reach paths across triplets with a rotation
794 applied (green: triplets with perturbations on Movement trials, magenta: triplets with perturbations on No-
795 Movement trials, solid lines: perturbation was a CW rotation, dashed lines: perturbation was a CCW
796 rotation). (**c**) STL across Movement (green) and No-Movement (magenta) triplets for all participants (n =
797 20). In the reference frame used here, positive changes in hand angle are CCW. Please refer to
798 Supplemental Table 1 for details on all statistical tests. (**d**) Group mean ± SEM Δhand angle values after
799 exposure to Movement (green) and No-Movement (magenta) trial perturbations. Positive Δ values indicate
800 that the change in hand angle proceeded opposite the direction of the perturbation (*i.e.,* the direction that

would counter the error, “Right-Way”). (**e**) Group mean of participants’ ratios of remembered STL to initial STL during Movement and No-Movement trials. (**f**) The relationship between Right-Way STL observed during Movement and No-Movement triplets. (**g**) As in (**f**), but for STL observed on trials where adaptation proceeded in the direction that would exacerbate the error (*i.e.*, the same direction as the perturbation applied, “Wrong Way”). Statistical significance (* = $p_{adj} < 0.05$; n.s. = $p_{adj} \geq 0.05$) is indicated. Abbreviations: STL – single-trial learning, CW – clockwise, CCW – counterclockwise, Δ – change in.

Figure 3. Effects of simulated errors when perturbations were never applied during Movement trials. (**a**) Schematic illustrating the relationship between movement and visual feedback on Movement trials during an experiment where visuomotor rotations (left) or error-clamps (right) were never applied during Movement trials. (**b**) An example participant’s mean ± SEM changes in reach paths across No-Movement triplets from studies in which non-zero rotations (left) and error-clamps (right) were never applied (solid lines: perturbation was CW, dashed lines: perturbation was CCW). (**c**) Boxplots showing STL in response to different directions of simulated errors (No-Movement triplets indicated in magenta) from rotation (left, $n = 24$) and error-clamp (right, $n = 37$) studies. (**d**) Estimated marginal means ± 95% confidence intervals from the linear mixed models fit to each participant’s STL performance summarized in (**c**). Asterisks indicate statistically significant differences. (**e**) Mean ± SEM relative hand angles on the two trials after a perturbation was presented on a No-Movement trial. Please refer to Supplemental Table 3 for detailed statistical results. Boxplot centers: median, notches: 95% confidence interval of the median, box edges: 1st and 3rd quartiles, whiskers: most extreme values within 1.5*IQR of the median. Statistical significance (* = $p_{adj} < 0.05$; n.s. = $p_{adj} \geq 0.05$) is indicated for selected comparisons. Abbreviations: STL – single-trial learning, CW – clockwise, CCW – counterclockwise, Δ – change in.

Supplemental information accompanying the submission of "Learning from the path not taken: Sensory prediction error computation and implicit motor adaptation proceed without movement"

Olivia A. Kim, Alexander D. Forrence, and Samuel D. McDougle

Contents:

2	Supplemental Figure 1
3	Supplemental Figure 2
4	Supplemental Figure 3
5	Supplemental Figure 4
6	Supplemental Figure Captions
10	Supplemental Table 1
11	Supplemental Table 2
12	Supplemental Table 3

Supplemental Figure 1

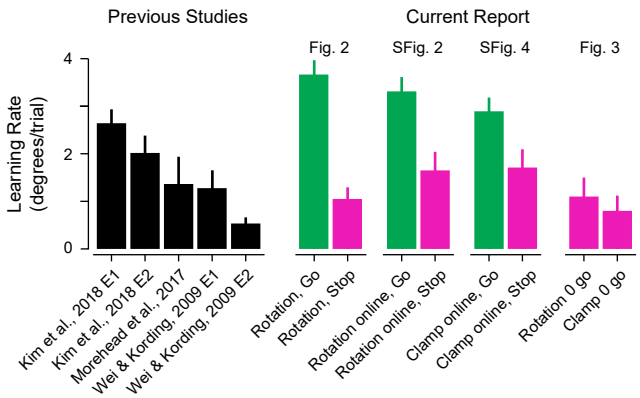

Supplemental Figure 2

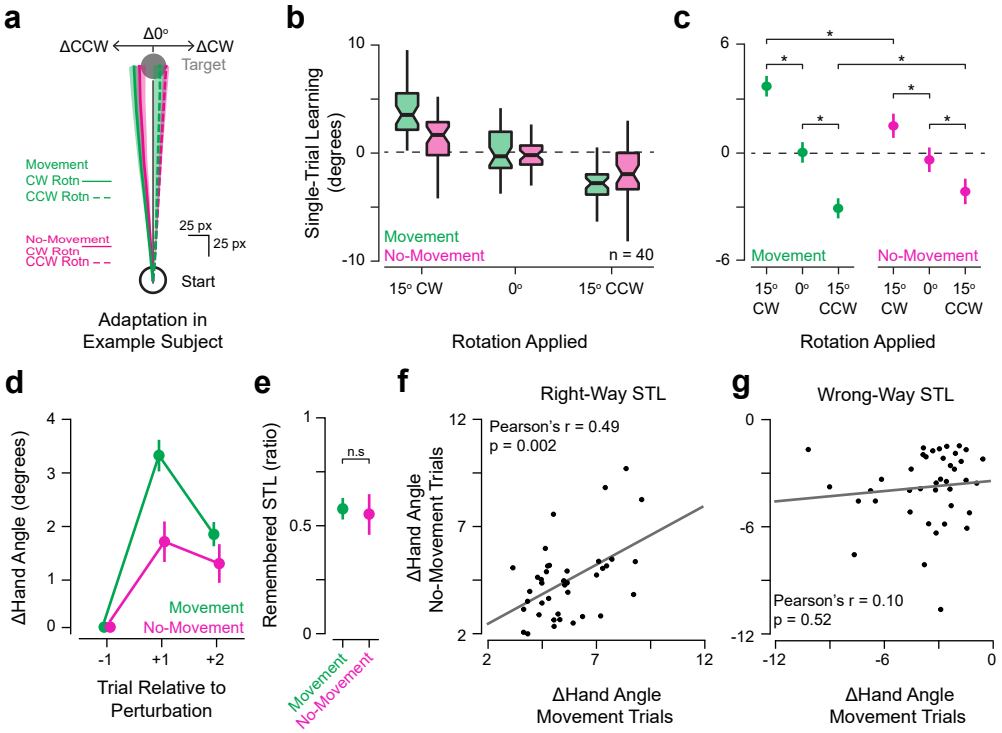

Supplemental Figure 3

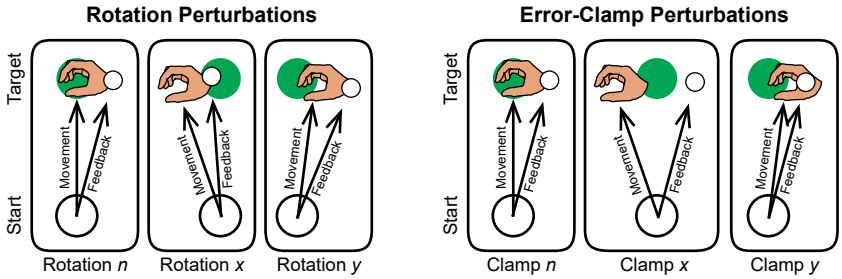

Supplemental Figure 4

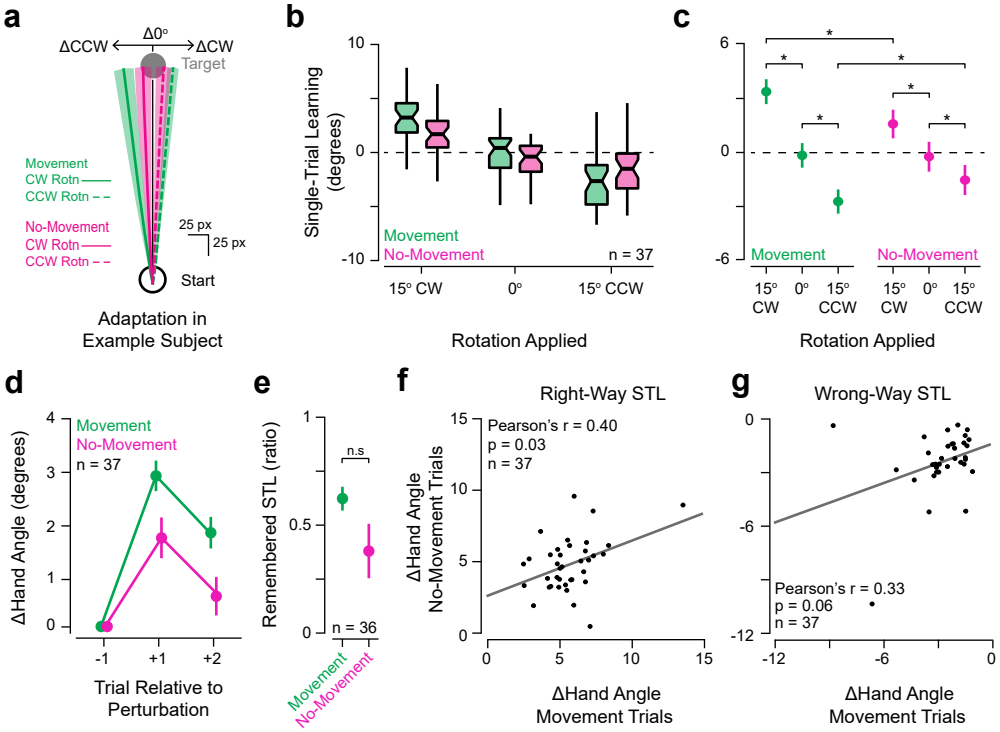

SUPPLEMENTAL FIGURE CAPTIONS

Supplemental Figure 1. Learning rates reported in the literature and observed in the current study. Learning rates for motor adaptation observed in previous studies are shown at left in black, and learning rates observed in each experiment in the current report are shown at the right, with data from Movement triplets shown in green and data from No-Movement triplets shown in magenta. Data are shown as mean ± SEM, and are shown for rotational/error clamp perturbations of 15°, with the exception of Wei & Kording, 2009 E2, where an 11° perturbation was applied. Papers referred to and their corresponding reference numbers: Kim et al., 2018[23]; Morehead et al., 2017[17]; Wei & Körding, 2009[27]. "Rotation, Go" and "Rotation, Stop" show data from the in-lab experiment where participants saw 15° rotated feedback on Movement trials (i.e., data from Fig. 2), "Rotation online, Go" and "Rotation online, Stop" show data from the online experiment where participants saw 0-15° rotated feedback on Movement trials (i.e., data from Supplemental Fig. 2). "Clamp online, Go" and "Clamp online, Stop" show data from the online experiment where participants saw 0-15° error-clamed feedback (i.e., data from Supplemental Fig., 4). "Rotation 0 go" and "Clamp 0 go" show data from the online experiments where participants saw 0° perturbed feedback on Movement trials. Abbreviations: E, experiment.

Supplemental Figure 2. Single-trial learning in response to errors on Movement and No-Movement trials during an online visuomotor adaptation task. (**a**) An example participant's mean ± SEM changes in reach paths across triplets (green: triplets with perturbations on Movement trials, magenta: triplets with perturbations on No-Movement trials, solid lines: perturbation was a CW rotation, dashed lines: perturbation was a CCW rotation). (**b**) Boxplot showing STL across Movement (green) and No-Movement (magenta) triplets for participants in an online version of the task described in Figure 1 ($n = 40$). (**c**) Estimated marginal means (EMMs) ± 95% confidence intervals from the linear mixed model (LMM) fit to participants' STL performance (summarized in **b**). The LMM (fixed effects: rotation [15° counterclockwise {CCW}, 0°, and 15° clockwise {CW}], movement condition [Movement, No-Movement], rotation x movement condition interaction; random effects: participant) revealed significant main effects of rotated cursor feedback ($F(2, 2223) = 136.46$, $p = 2.2 \times 10^{-16}$, *partial* $R^2 = 0.11$) and movement condition ($F(1, 2248) = 4.74$, $p = 0.03$, *partial* $R^2 = 0.002$), as well as a significant interaction ($F(2, 2229) = 12.40$, $p = 4.41 \times 10^{-6}$, *partial* $R^2 = 0.01$).

Post-hoc pairwise comparisons of the EMMs from the model support the claim that rotated feedback induced a statistically significant degree of STL on both Movement (0° vs 15° CW: $t(2227) = 9.14$, $p_{adj} = 6.39 \times 10^{-19}$, *Cohen's d* = 0.61; 0° vs 15° CCW: $t(2220) = 7.81$, $p_{adj} = 2.61 \times 10^{-14}$, *Cohen's d* = 0.52) and No-Movement trials (0° vs 15° CW: $t(2225) = 3.92$, $p_{adj} = 1.39 \times 10^{-4}$, *Cohen's d* = 0.31; 0° vs 15° CCW: $t(2229) = 3.56$, $p_{adj} = 4.84 \times 10^{-4}$, *Cohen's d* = 0.29). Adaptation in the presence of a rotation was significantly greater in Movement trials than No-Movement trials for CW ($t(2238) = 4.98$, $p_{adj} = 1.26 \times 10^{-6}$, *Cohen's d* = 0.37) and CCW rotations ($t(2239) = 2.06$, $p_{adj} = 0.04$, *Cohen's d* = 0.15). (**d**) Group mean ± SEM change in (Δ) hand angle after exposure to Movement (green) and No-Movement (magenta) triplets' perturbations. Positive Δ values indicate that the change in hand angle proceeded opposite the direction of the perturbation (*i.e.,* in the direction that would counter the error). (**e**) Group mean ± SEM ratio of remembered STL to STL. Remembered STL was statistically significantly greater than 0 for both Movement (one-sample signed-rank test: $V = 819$, $p_{adj} = 1.09 \times 10^{-11}$, $r = 0.87$) and No-Movement triplets ($V = 769$, $p_{adj} = 9.69 \times 10^{-8}$, $r = 0.76$), but remembered STL did not significantly differ between movement conditions (paired-samples signed-rank test: $V = 441$, $p_{adj} = 0.68$). (**f**) Scatter plot showing the relationship between individual subjects' STL amplitude in the direction opposite the rotation on Movement and No-Movement trials. When we considered instances of STL in the direction that would compensate for the observed error (update opposite rotation, "Right-Way"), within-subject changes in hand angle were correlated between Movement and No-Movement trials (*Pearson's r* = 0.49, $p_{adj} = 0.002$). (**g**) As in **f**, but showing data from trials with changes in hand angle in the direction that would exacerbate the observed error (update in direction of rotation, "Wrong-Way"). These ΔHand Angle values were uncorrelated between Movement and No-Movement trials (*Pearson's r* = 0.10, $p_{adj} = 0.52$). These observations support the idea that the same learning process may underlie adaptive single-trial learning events in response to errors on both kinds of trials, while maladaptive changes in hand-angle may be attributable to potential sources of random noise. Boxplot centers: median, notch: 95% confidence interval of the median, box edges: 1st and 3rd quartiles, whiskers: most extreme value within 1.5*interquartile range of the median. Statistical significance (* = $p < 0.05$; n.s. = $p \geq 0.05$) is. Abbreviations: STL – single-trial learning, Δ – change, CW – clockwise, CCW – counterclockwise.

Supplemental Figure 3. Schematics illustrating the difference between rotation and error-clamp perturbations. Diagrams showing the relationship between hand and cursor feedback movement directions under rotational error regimes (left) and error-clamp regimes (right). When rotational perturbations are applied to cursor feedback, the cursor's movement direction is contingent upon the participant's movement direction, although there is an experimenter-induced offset. If a rotation is consistently applied, participants explicit aiming strategies are a viable supplement for imperfect implicit motor performance. When error-clamp perturbations are applied to cursor feedback, the cursor travels in a fixed direction, regardless of the direction that the hand travels, rendering explicit aiming strategies useless. Thus, error-clamp perturbations are often used in studies attempting to isolate implicit motor adaptation processes.

Supplemental Figure 4. Single-trial learning in response to errors on Movement and No-Movement trials with error-clamped feedback or simulated errors. (**a**) An example participant's mean ± SEM changes in reach paths across triplets (green: triplets with perturbations on Movement trials, magenta: triplets with perturbations on No-Movement trials, solid lines: perturbation was a CW error-clamp, dashed lines: perturbation was a CCW error-clamp). (**b**) Boxplot showing STL across Movement (green) and No-Movement (magenta) triplets for participants (n = 37) in an online experiment where cursor feedback was error-clamped on Movement trials. (**c**) Estimated marginal means (EMMs) ± 95% confidence intervals from the linear mixed model (LMM) fit to participants' STL performance (summarized in **b**). The LMM (fixed effects: rotation [15° counterclockwise {CCW}, 0°, and 15° clockwise {CW}], movement condition [Movement, No-Movement], error-clamp x movement condition interaction; random effects: participant) revealed significant main effects of error-clamped cursor feedback ($F(2, 1829) = 79.46$, $p = 2.2 \times 10^{-16}$, *partial* $R^2 = 0.08$) and an interaction between error-clamp and movement condition ($F(2, 1832) = 8.45$, $p = 0.0002$, *partial* $R^2 = 0.0003$), although there was no main effect of movement condition ($F(1, 1844) = 0.60$, $p = 0.44$). Post-hoc comparisons of the EMMs from the model revealed significant STL in response to non-zero error-clamped feedback on both Movement (0° vs 15° CW: $t(1827) = 7.55$, $p_{adj} = 3.08 \times 10^{-13}$, *Cohen's d* = 0.56; 0° vs 15° CCW: $t(1828) = 5.57$, $p_{adj} = 8.84 \times 10^{-8}$, *Cohen's d* = 0.41) and No-Movement trials (0° vs 15° CW: $t(1830) = 3.21$, $p_{adj} = 0.002$, *Cohen's d* = 0.29; 0° vs 15° CCW: $t(1832) = 2.25$, $p_{adj} = 0.03$,

Cohen's d = 0.22). Adaptation in the presence of a 15° error-clamp was significantly greater on Movement trials than No-Movement trials for CW ($t(1846) = 3.49$, $p_{adj} = 0.0009$, *Cohen's d* = 0.29) and CCW clamps ($t(1846) = 2.29$, $p_{adj} = 0.03$, *Cohen's d* = 0.19). Please refer to Supplemental Table 2 for further details on post-hoc comparisons in this panel. (**d**) Group mean ± SEM change in (Δ) hand angle one and two trials after exposure to Movement (green) and No-Movement (magenta) triplets' perturbations. Positive Δ values indicate that the change in hand angle proceeded opposite the direction of the perturbation (*i.e.,* in the direction that would counter the error). (**e**) Remembered STL shown as the ratio of relative hand angle 2 trials after experiencing a perturbation to the relative hand angle 1 trial after the perturbation (STL). Remembered STL was significantly greater than 0 after both Movement (green; one-sample t-test: $t(36) = 11.31$, $p_{adj} = 6.23 \times 10^{-13}$, *Cohen's d* = 1.86) and No-Movement triplets (magenta, one-sample signed-rank test: $V = 579$, $p_{adj} = 5.95 \times 10^{-5}$, $r = 0.64$), but did not exhibit statistically significant differences between movement conditions (paired t-test: $t(35) = 1.71$, $p_{adj} = 0.09$). Remembered STL on No-Movement trials could not be computed for one participant, so $n = 36$ instead of 37 in this panel. (**f**) Scatter plot showing the relationship between individual subjects' STL amplitude in the direction opposite the error-clamp on Movement and No-Movement trials (i.e., the "Right-Way"). Right-way changes in hand angle were correlated between Movement and No-Movement trials (*Pearson's r* = 0.40, $p_{adj} = 0.03$). (**g**) As in (**f**), but showing data from trials on which STL proceeded in the same direction as the error-clamp (*i.e.*, the "Wrong-Way"). Wrong-Way changes in hand angle were not statistically significantly correlated between Movement and No-Movement trials ($r = 0.33$, $p_{adj} = 0.06$). These observations support the idea that the same learning process may underlie adaptive single-trial learning events in response to errors on both kinds of trials, while maladaptive changes in hand-angle may be attributable to potential sources of random noise. Boxplot centers: median, notch: 95% confidence interval of the median, box edges: 1st and 3rd quartiles, whiskers: most extreme value within 1.5*interquartile range of the median. Statistical significance (* = $p < 0.05$; n.s. = $p \geq 0.05$) is indicated for selected comparisons. Abbreviations: STL – single-trial learning, Δ – change, CW – clockwise, CCW – counterclockwise.

SUPPLEMENTAL TABLES

Supplemental Table 1.

Pairwise post-hoc comparisons between estimated marginal means in Supplemental Fig. 2c

Group 1		Group 2		Est. Diff.	t	df	FDR-adjusted p	Cohen's d
Trial Type	Rotation	Trial Type	Rotation					
M	0°	M	15° CW	-3.67°	-9.14	2227	* 6.39×10^{-19}	-0.61
M	0°	M	15° CCW	3.09°	7.81	2220	* 2.60×10^{-14}	0.52
M	15° CW	M	15° CCW	6.76°	17.08	2223	* 1.31×10^{-60}	1.13
No-M	0°	No-M	15° CW	-1.88°	-3.92	2225	* 0.0001	-0.31
No-M	0°	No-M	15° CCW	1.75°	3.56	2229	* 0.0005	0.29
No-M	15° CW	No-M	15° CCW	3.64°	7.41	2231	* 3.86×10^{-13}	0.61
M	0°	No-M	0°	0.41°	0.93	2240	0.35	--
M	15° CW	No-M	15° CW	2.20°	4.98	2238	* 1.25×10^{-6}	0.37
M	15° CCW	No-M	15° CCW	-0.93°	-2.06	2239	* 0.04	-0.15

Note. Abbreviations: M – Movement; No-M – No-Movement; Est. Diff. – Estimated Differences in degrees. Note that degrees of freedom pertain to the inputs to the LMM and are estimated using the Kenward-Rogers approach. Statistically significant p-values are indicated with asterisks. * $p < 0.05$.

Supplemental Table 2.

Pairwise post-hoc comparisons between estimated marginal means in Supplemental Fig. 4c

Group 1		Group 2		Est. Diff.	t	df	FDR-adjusted p	Cohen's d
Trial Type	Rotation	Trial Type	Rotation					
M	0°	M	15° CW	3.54°	-7.55	1827	* 3.08×10^{-13}	-0.56
M	0°	M	15° CCW	2.57°	5.57	1828	* 8.84×10^{-8}	0.41
M	15° CW	M	15° CCW	6.11°	13.14	1828	* 8.51×10^{-37}	0.97
No-M	0°	No-M	15° CW	-1.81°	-3.21	1830	* 0.002	-0.29
No-M	0°	No-M	15° CCW	1.29°	2.25	1832	* 0.03	0.20
No-M	15° CW	No-M	15° CCW	3.10°	5.46	1833	* 1.24×10^{-7}	0.49
M	0°	No-M	0°	0.08°	0.16	1846	0.87	--
M	15° CW	No-M	15° CW	1.81°	3.49	1846	* 0.0009	0.29
M	15° CCW	No-M	15° CCW	-1.19°	-2.28	1846	* 0.03	-0.19

Note. Abbreviations: M – Movement; No-M – No-Movement; Est. Diff. – Estimated Differences in degrees. Note that degrees of freedom pertain to the inputs to the model and are estimated using the Kenward-Rogers approach. Statistically significant p-values are indicated with asterisks. * $p < 0.05$.

Supplemental Table 3.

Pairwise post-hoc comparisons between estimated marginal means in Fig. 3

Group 1		Group 2		Est. Diff.	t	df	FDR-adjusted p	Cohen's d
Trial Type	Rotation	Trial Type	Rotation					
0° Rotation Applied on Movement Trials								
No-M	15° CCW	No-M	15° CW	2.45°	4.80	557	* 2.07×10^{-6}	0.40
0° Error-Clamped Feedback on Movement Trials								
No-M	15° CCW	No-M	15° CW	2.37°	4.32	805	* 0.0001	0.37
No-M	15° CW	No-M	0°	1.36°	2.48	801	* 0.020	0.21
No-M	15° CCW	No-M	0°	1.01°	1.83	800	0.067	--

Note. Abbreviations: No-M – No-Movement; Est. Diff. – Estimated Differences in degrees. Note that degrees of freedom pertain to the inputs to the model and are estimated using the Kenward-Rogers approach. Statistically significant p-values are indicated with asterisks. * $p < 0.05$.